

# Lawrence Berkeley National Laboratory

## Recent Work

### Title

PERMEATION OF MDNATOMIC GASES THROUGH ALUMINUM OXIDE

### Permalink

<https://escholarship.org/uc/item/6bb3b4x5>

### Author

Edwards, Richard Hugh.

### Publication Date

1966-08-25

**University of California**  
**Ernest O. Lawrence**  
**Radiation Laboratory**

PERMEATION OF MONATOMIC GASES THROUGH ALUMINUM OXIDE

**TWO-WEEK LOAN COPY**

*This is a Library Circulating Copy  
which may be borrowed for two weeks.  
For a personal retention copy, call  
Tech. Info. Division, Ext. 5545*

## **DISCLAIMER**

This document was prepared as an account of work sponsored by the United States Government. While this document is believed to contain correct information, neither the United States Government nor any agency thereof, nor the Regents of the University of California, nor any of their employees, makes any warranty, express or implied, or assumes any legal responsibility for the accuracy, completeness, or usefulness of any information, apparatus, product, or process disclosed, or represents that its use would not infringe privately owned rights. Reference herein to any specific commercial product, process, or service by its trade name, trademark, manufacturer, or otherwise, does not necessarily constitute or imply its endorsement, recommendation, or favoring by the United States Government or any agency thereof, or the Regents of the University of California. The views and opinions of authors expressed herein do not necessarily state or reflect those of the United States Government or any agency thereof or the Regents of the University of California.

UNIVERSITY OF CALIFORNIA

Lawrence Radiation Laboratory  
Berkeley, California

AEC Contract No. W-7405-eng-48

PERMEATION OF MONATOMIC GASES THROUGH ALUMINUM OXIDE

Richard Hugh Edwards  
(M.S. Thesis)

August 25, 1966

PERMEATION OF MONATOMIC GASES THROUGH ALUMINUM OXIDE

Contents

Abstract . . . . .	v
I. Introduction . . . . .	1
II. Literature Survey . . . . .	3
III. Experimental Procedure . . . . .	6
A. Specimens . . . . .	6
1. Specimen Shape and Composition . . . . .	6
2. Production of Permeation Section . . . . .	9
3. Hot-Pressing of Specimen and Plug . . . . .	10
B. Apparatus . . . . .	13
1. Furnace Arrangement . . . . .	13
2. Gas Pressurizing System . . . . .	17
3. Flow Detection System . . . . .	17
C. Test Procedure . . . . .	18
1. General Procedure . . . . .	18
2. Helium Procedure . . . . .	18
3. Argon Procedure . . . . .	19
D. Microscopic Examination . . . . .	21
IV. Experimental Results . . . . .	24
A. Helium Permeation Constants . . . . .	24
B. Helium Activation Energies . . . . .	24
C. Argon Permeation Runs . . . . .	28

V. Discussion . . . . .	29
VI. Summary and Conclusions . . . . .	34
Acknowledgments . . . . .	35
Appendices . . . . .	36
References . . . . .	40

PERMEATION OF MONATOMIC GASES THROUGH ALUMINUM OXIDE

Richard Hugh Edwards

Inorganic Materials Research Division, Lawrence Radiation Laboratory,  
and Department of Mineral Technology, College of Engineering,  
University of California, Berkeley, California

August 25, 1966

ABSTRACT

Permeation studies of helium and argon through commercial alumina bodies were made. Permeation occurred through thin diamond ground cylindrical sections. Flow rates through the specimen were measured by a residual gas analyzer. Helium and argon pressures of 380 to 1010 mm Hg over temperatures from 783 to 1539°C were used for specimens containing 99.5 and 94 weight percent  $\text{Al}_2\text{O}_3$ . Permeation constants and activation energies were calculated.

Helium permeation constants up to  $1.4 \times 10^{11}$  and  $8.1 \times 10^9$  atoms/sec cm atm and average activation energies of  $13.6 \pm 2.3$  and  $13 \pm 1.7$  Kcal/mole were found for the 94 and 99.5% alumina ceramics, respectively. No argon flow through the specimens was detected at pressures up to 1010 mm Hg. The limit of detectability of the apparatus fixes K values for argon permeation at less than  $2 \times 10^9$  atoms/sec cm atm in the temperature range studied. Helium diffusion along continuous glassy paths was thought to be responsible for flow through both alumina bodies.

## I. INTRODUCTION

In recent years the number of applications calling for ceramic materials to be used at high temperatures under vacuum or controlled atmospheric conditions has increased. Alumina is used as an envelope for high power electronic tubes which must operate at elevated temperatures. Here the ceramic body must maintain its strength under pressure differentials at temperature and prevent gases from entering the inside of the tube. Use of a translucent alumina envelope impermeable to sodium vapors has enabled engineers to produce a sodium vapor bulb which operates at substantially higher temperatures than a normal filament bulb. This has led to large increases in total light output and efficiency of operation.

Knowledge of the degree and mechanism of permeation of gases through these materials is necessary, yet to date little work has been done in this area.

From a practical standpoint, measurements of the permeability of various commercial ceramic bodies at high temperatures are needed to permit use of the materials available now at their maximum capabilities. On the other hand, fundamental studies of the mechanisms and effects of impurities and grain size must also be made. Once the fundamental rate controlling factors for permeation are known and understood, new materials may be produced with any desired permeation characteristics.

It is the lack of information on permeation rates through alumina materials which prompted this study. The objective of the investigation was to determine the permeation characteristics of different commercial



grades of alumina using helium and argon as the gaseous species. From calculations of the activation energies, an attempt was made to deduce the mechanism of flow through the body.

## II. LITERATURE SURVEY

Few studies have been made on the permeation of gases through alumina. Roberts, et al.<sup>1,2</sup> investigated permeation of oxygen, nitrogen and argon through extruded alumina tubes at temperatures of 1500 to 1700°C. Little argon and nitrogen permeation was observed. Kinetics of the oxygen permeation indicated a solid state diffusion process. These tubes, studied by microscopic techniques, showed formation of a dense skin-like layer at the outside of the tube and considerable connected porosity in the remainder of the body.<sup>3</sup> It is believed the skin formation may be related to preferred orientation imparted to the platy alumina particles during forming by slip casting or extrusion.<sup>4</sup>

Work has been done to suggest that volatilization of impurities also has a large effect on the permeation characteristics of alumina<sup>5</sup> and mullite materials. In the case of mullite, loss or migration of the glassy phase from the hot zone at temperatures above 1600°C caused formation of a dense mullite layer which lowered the observed permeation rates.<sup>5</sup> Deterioration--the sudden loss of impermeability after tens of hours at high temperatures resulting from the formation of channels through the body--may be caused by the loss of impurities in alumina bodies. In a 99.3% Al<sub>2</sub>O<sub>3</sub> body, loss of silica was observed with formation of channels along so-called three grain edges.<sup>4</sup> Deterioration has also been associated with loss of  $\alpha$ -Al<sub>2</sub>O<sub>3</sub>, or in another experiment with iron, calcium, and magnesium.<sup>6</sup>

Most permeation rates measured at temperatures used in the studies by Roberts and his co-workers<sup>1-6</sup> are transient permeation rates. Tubes apparently impermeable at first lose impermeability to gaseous species

with time. At those very high temperatures ( $>1600^{\circ}\text{C}$ ) drastic changes are continually occurring in the microstructures. Microstructural changes in turn control the permeation rates. In many cases true steady permeation has never been reached and cannot be reached since deterioration and failure occur first.

Volk<sup>7</sup> has studied the permeation of oxygen through polycrystalline and single crystal alumina at temperatures about  $1700^{\circ}\text{C}$ . No oxygen permeation through the single crystal material to within  $10^{\circ}\text{C}$  of its melting point was detected. As-received polycrystalline tubes exhibited erratic and non-reproducible behavior. Samples reached constant reproducible values after heat treatments of 4 to 6 hours at  $1830$  to  $1915^{\circ}\text{C}$  which would help stabilize the microstructure. The effects of up to 6% closed porosity on permeation rates was found to be negligible. Activation energies of 105 to 135 Kcal/mole were found for oxygen permeation.

Campbell<sup>8</sup> investigated helium diffusion through polycrystalline and single crystal alumina at low temperatures ( $25-900^{\circ}\text{C}$ ). He reports flow occurred over the entire temperature range. Diffusion coefficients of  $10^{-7}$   $\text{cm}^2/\text{sec}$  to  $10^{-10}$   $\text{cm}^2/\text{sec}$ , varying inversely with the density of the body, and an activation energy of 3.0 Kcal/mole were found for the polycrystalline alumina.

Campbell's results were not substantiated by Stansfield<sup>9</sup> who found no permeation of helium through polycrystalline alumina samples at temperatures to  $900^{\circ}\text{C}$ . Rose,<sup>10</sup> however, found permeation occurring at temperatures between  $1000$  and  $1500^{\circ}\text{C}$ . Permeation coefficients in the  $10^9$  atoms/sec cm atm range and activation energies of about 13

Kcal/mole were reported. Permeation rates decreased with successive heat treatments and an increase in activation energy was suspected. No obvious microstructural changes in the tested specimens were seen.

Studt<sup>11</sup> investigated stress-enhanced helium permeation through high alumina bodies at room temperature. Helium bursts were seen during the application of stress to the permeation membrane. It was thought that stress-enhanced flow was occurring through interconnected pores.

In later work Atallah<sup>12</sup> found that diamond grinding could form microcracks to a depth of at least 0.005 inches in a permeation section. These could be healed by heating the specimen to a temperature dependent on the composition and previous processing of the body. It is most probable that the bursting phenomenon observed by Studt was the result of flow through microcracks induced during the grinding of his specimens.

Fryer and Roberts<sup>13</sup> have studied alumina materials subjected to axial tensile stresses at high temperatures (1400-1600°C) where microstructural changes and creep phenomena might be expected to play a large role in determining the permeation characteristics. Samples originally impermeable to helium at a given temperature showed time dependent leakage that was highly sensitive to the applied stress. Leakage was also dependent on the amount of extension at a given stress. Flow was probably through channels 1 to 5 microns in diameter which developed in the material during extensive deformation.

The work in this investigation follows that of Rose.<sup>10</sup> The detection system was modified to allow monitoring of all gaseous species. Both helium and argon were used as the permeating species through tubes of two different alumina compositions.

### III. EXPERIMENTAL PROCEDURE

#### A. Specimens

##### 1. Specimen Shape and Composition

Tubes 15 in. long, 3/4 in o.d. and 5/16 in. i.d. with a collar at one end 1-1/8 in. o.d. by 1 in. long were fabricated by isostatic pressing and high temperature sintering in air. The dimensions of the as-received tubes are shown in Fig. 1(a). Tubes containing nominal alumina contents of 99.5 and 94% were made by the supplier.\* Alumina rods of the same two compositions 1-1/8 in. o.d. by 8 in. long were also supplied.

The thermal history and physical properties of the as-received tubes are given in Table I. A semi-quantitative emission spectrographic analysis was made on each composition. These results are given in Table II.

Table I. Thermal history and physical properties of  
as-received specimen tubes

Tube #	Nominal Al <sub>2</sub> O <sub>3</sub> content (%)	Firing temp (°C)	Firing time (hrs.)	Apparent density (g/cc)	Apparent porosity (%)
1	94	1650	3	3.66	8.1
2	99.5	1765	3	3.85	3.4

\* Western Gold and Platinum Company, Belmont, California

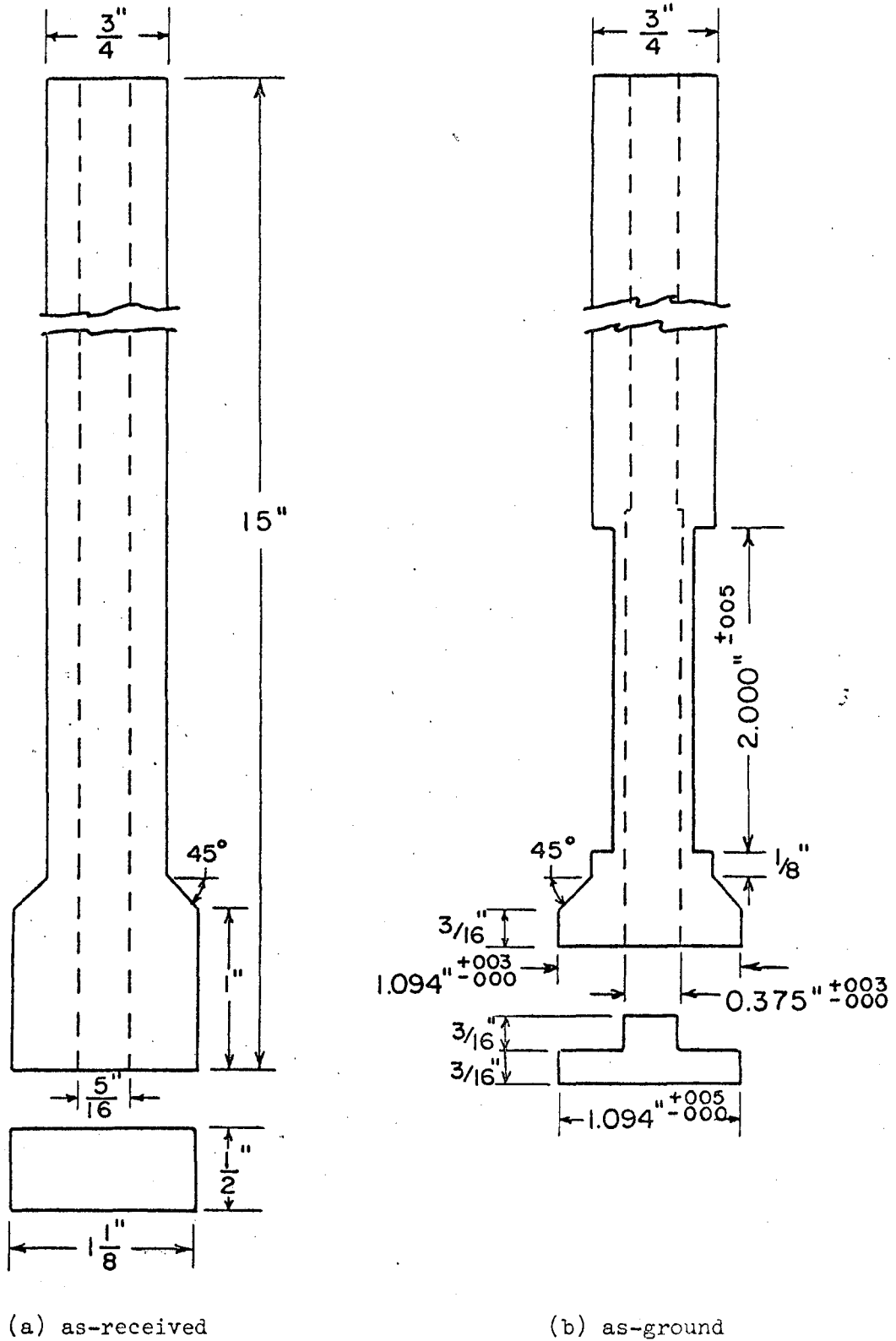


Fig. 1. Alumina specimen tubes and end plugs as-received and as-ground.

Table II. Spectrographic analysis of materials,  
by weight percent

Compound	Nominal alumina content (%)	
	94	99.5
MgO	0.45	0.4
CaO	0.5	0.03
SiO <sub>2</sub>	4.	0.25
Fe <sub>2</sub> O <sub>3</sub>	0.2	0.08
B <sub>2</sub> O <sub>3</sub>	0.02	0.03
MnO	0.002	<0.001
Ga <sub>2</sub> O <sub>3</sub>	0.02	0.02
CuO	0.003	0.001
TiO <sub>2</sub>	0.05	0.01
Cr <sub>2</sub> O <sub>3</sub>	0.004	<0.001
BaO	0.001	0.002
Na <sub>2</sub> O	<0.1	<0.1
ZnO	<0.1	<0.1
ZrO <sub>2</sub>	<0.005	<0.005
NiO	<0.003	<0.003
VO	<0.003	<0.003
Al <sub>2</sub> O <sub>3</sub>	>94.5	>99.0

## 2. Production of Permeation Section.

When performing permeation experiments it is important to have a permeation section which is both uniform in thickness and well defined in area. It is difficult to produce a tube with a uniform wall thickness in the as-fired condition. By diamond-grinding both the internal and external surfaces of the tube, however, a section of desired area and thickness can be produced.

A diamond wheel was used to grind both the i.d. and o.d. surfaces of the tubes to produce a permeation section 2 in. long with a wall thickness of approximately 0.035 inches. The wall thickness of the remaining portions of the tube is about an order of magnitude greater than that of the section.

Internal diamond grinding must of necessity be done near one end of the tube, thus placing the section near that end.

To facilitate testing of the specimen, it is necessary to seal the end of the tube near the section. The sealing was done by vacuum hot-pressing an alumina plug of the same composition onto that end. The plugs were ground from the alumina rods made by the supplier. A layer of fine alumina powder was placed between the plug and the tube and this was densified to produce a nearly pore free, fine-grained seal.

The dimensions and section configuration of the ground tube may be seen in Fig. 1(b). The 45° angle seen in Fig. 1(b) was used to prevent large shearing forces from acting on the alumina body. The angle was also diamond ground to provide a uniform die contact area during the hot-pressing operation.



The dimensions of the ground permeation sections for each of the specimen tubes are given in Table III.

Table III. Dimensions of ground permeation sections

Spec. #	Compo- sition (%Al <sub>2</sub> O <sub>3</sub> )	Inside radius, a (cm)	Outside radius, b (cm)	Length, l (cm)	Wall thick- ness, t (cm x 10 <sup>2</sup> )	Area, A (2πal cm <sup>2</sup> )
1	94	0.477	0.569	5.08	9.21	15.24
2	99.5	0.479	0.571	5.08	9.27	15.28

### 3. Hot-pressing of Specimen and Plug.

Alumina components were first successfully hot-pressed together by Budworth et al.<sup>14</sup> who sealed alumina tubes at 1700°C and 1000 psi. In this investigation the plug and tube were joined in a manner similar to that used by Rose<sup>10</sup> who vacuum hot-pressed alumina components together at 1300-1350°C with a pressure of 600 psi held for 70-80 min. Using this technique, Rose avoided the large amount of grain growth noted by Budworth and the original grain structure in the permeation section of his specimens was retained.

Prior to hot-pressing, the plug and the end of the tube were lapped with six micron diamond paste to insure an intimate contact between the components.

Linde A alumina powder was washed several times with isopropyl alcohol and a slip containing about 1 part Linde A and 9 parts isopropyl alcohol by volume was prepared. The isopropyl alcohol treatment was found to aid in the densification process at temperature.<sup>15</sup>

The plug was placed in a small Petri dish. The prepared slip was then poured over the plug until the top was just covered. The plug was removed from the dish after approximately 30 minutes when the majority of the alumina particles had settled out of suspension. The coating thickness at that time was roughly 0.040 inches.

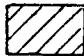


After at least six hours of air drying at room temperature, the alumina layer on that part of the plug not in contact with the specimen surface during pressing was removed. The coated plug was then ready for loading in the die.

The die was bored from a single piece of molybdenum. Using the configuration shown in Fig. 2 the only force directly on the permeation section during hot-pressing is the weight of the tube itself. Once the powder surface is mated with the end of the tube in the die it is extremely important that the integrity of the joint is not disturbed before the pressing operation begins.

The vacuum hot-press used has been described elsewhere by Rossi.<sup>15</sup> It is capable of temperatures to 1550°C and pressures of 10,000 psi.

The die assembly was mounted in the press and the press was evacuated to  $10^{-4}$  mm Hg or lower. An initial pressure of 1000 psi was applied to the powder surface and released. This was done to consolidate the layer and force out any extra powder present.

The 99.5%  $\text{Al}_2\text{O}_3$  specimen was heated to 1350-1365°C over a period of two hours under an applied pressure of 200 psi. At temperature, a pressure of 850-900 psi was applied and held for two hours. The pressure was then reduced to about 300 psi, after which the specimens were cooled to room temperature.

-  MOLYBDENUM
-  ALUMINA
-  GRAPHITE

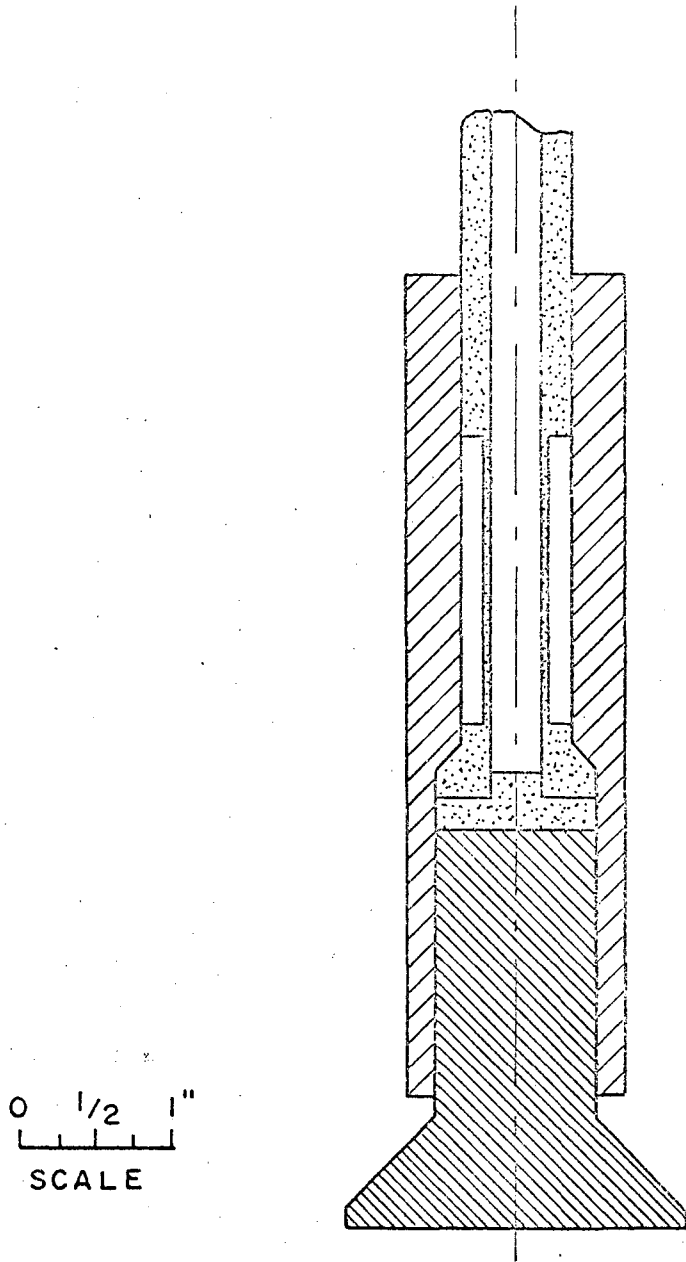


Fig. 2. Hot-press die assembly with plug and tube in place.

Using the preceding temperature-pressure schedule with the 94% Al<sub>2</sub>O<sub>3</sub> tube, severe deformation occurred. The specimen deformed at that point where the i.d. portion of the 45° molybdenum shoulder contacted the alumina surface. Deformation started after approximately 45 minutes at pressure and temperature (see Fig. 3). Deformation was prevented and leak tight seals obtained with the 94% Al<sub>2</sub>O<sub>3</sub> specimens if the pressure was reduced to 600 psi, the temperature reduced to 1350°C and the pressing time increased to 2 hours and 45 minutes.

After hot-pressing, all specimens were heated in an oxidizing atmosphere to a high temperature to heal any microcracks formed during the diamond grinding process. Specimens of 99.5% Al<sub>2</sub>O<sub>3</sub> were heated to 1500°C for four hours; 94% Al<sub>2</sub>O<sub>3</sub> samples to 1450°C for four hours.

A helium leak detector was used to check the fired specimens at room temperature for leaks. Specimens were also leak tested at temperature with the residual gas analyzer prior to prolonged testing.

#### B. Apparatus

A schematic representation of the apparatus is given in Fig. 4.

##### 1. Furnace Arrangement.

An alumina protection tube containing the permeation specimen (see Fig. 5) was mounted in a vacuum furnace with a hot zone of approximately four inches in length.

The temperature of the permeation section was measured by a Pt.-Pt 10% Rh. thermocouple within the specimen tube midway along the section. The temperature variation along the two-inch length of the section was approximately 20° at 1500°C.



ZN-5896

Fig. 3. Deformed 94% Al<sub>2</sub>O<sub>3</sub> specimen after hot-pressing.

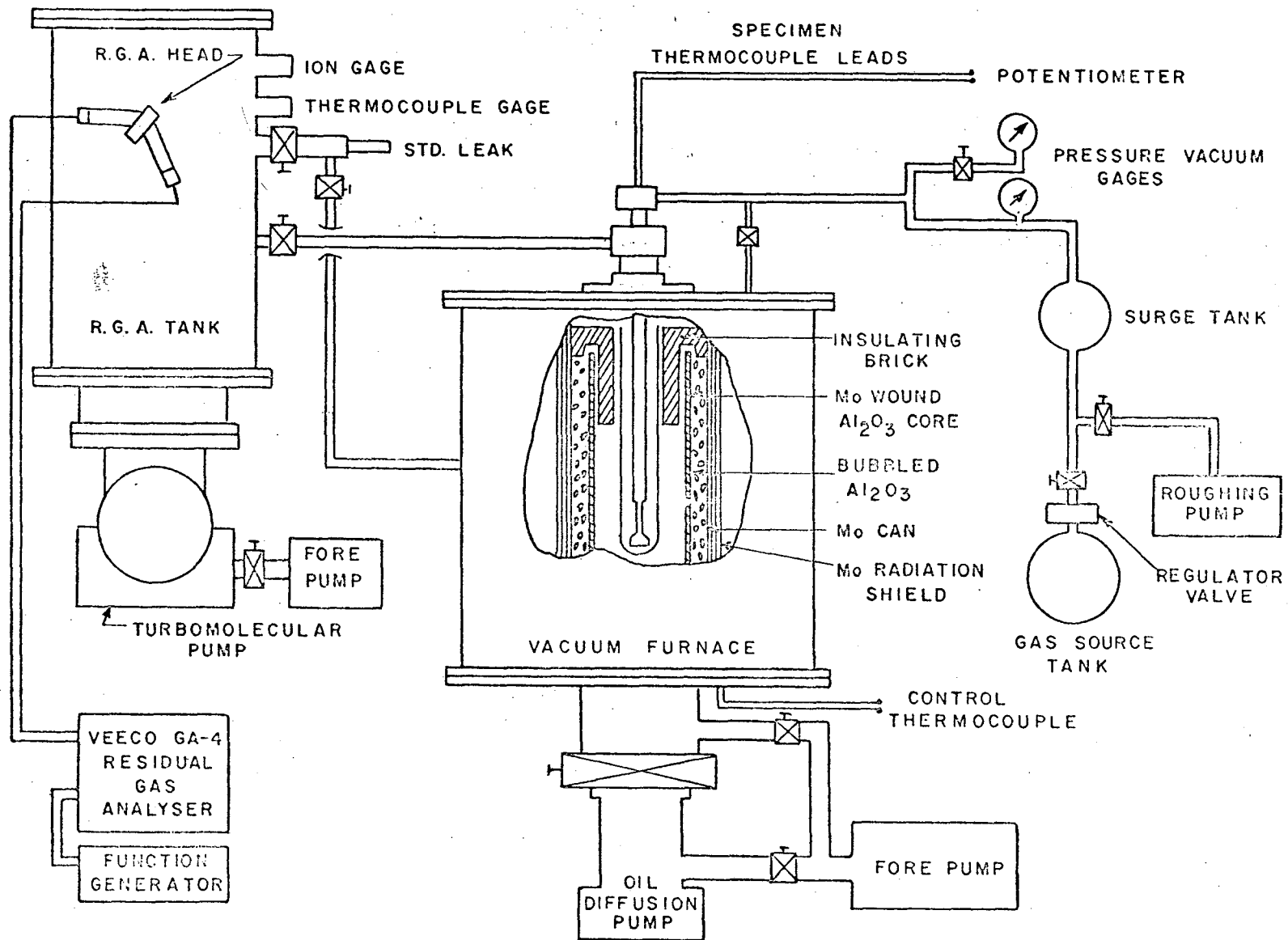


Fig. 4. Schematic representation of the apparatus.

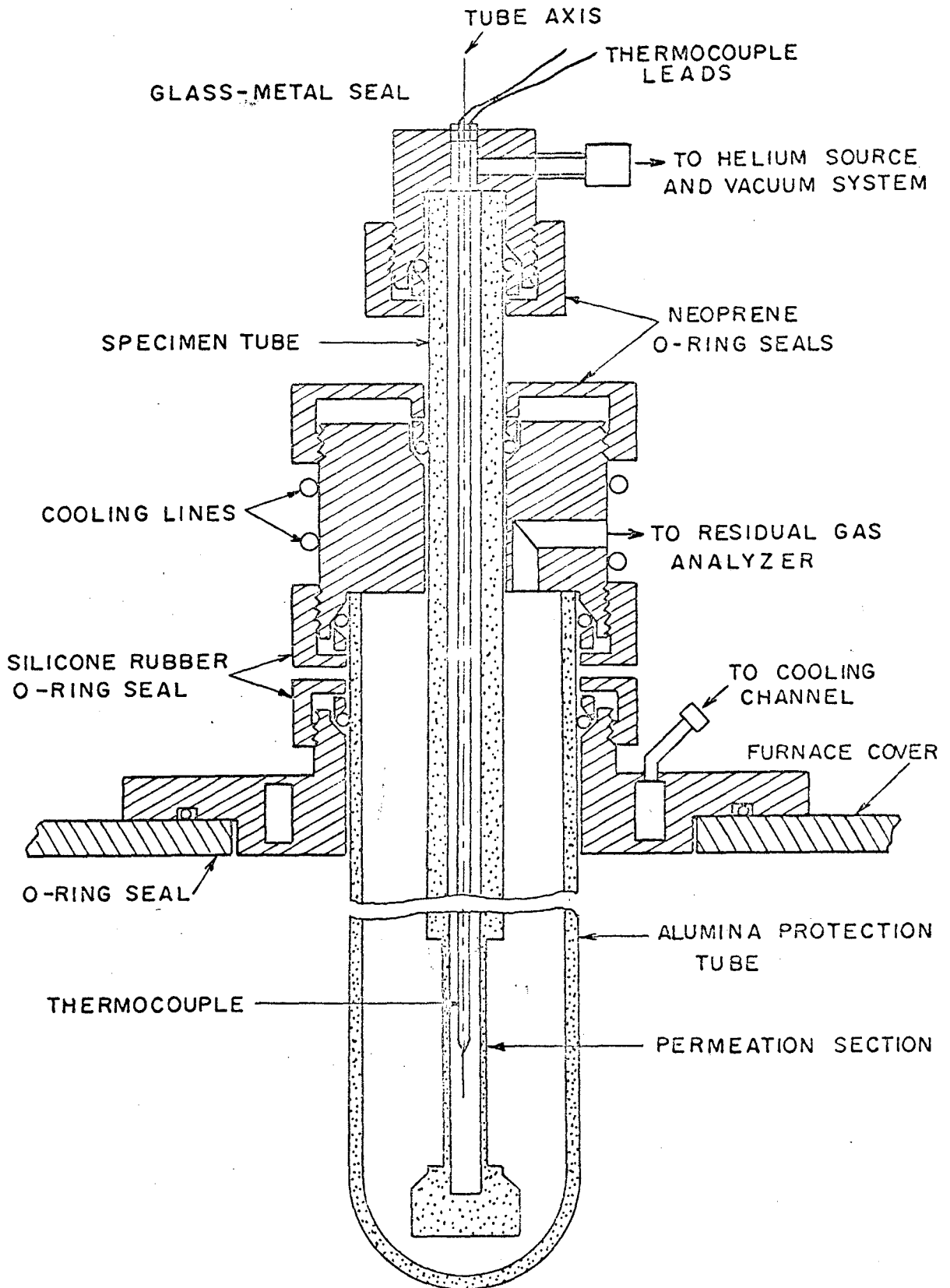


Fig. 5. Specimen and protection tube assembly.

## 2. Gas Pressurizing System

The pressure inside the specimen was varied by evacuating the system to 30 in. Hg and introducing helium or argon through a regulator-valve combination (see Fig. 4). Pressure in the system was measured with pressure-vacuum gages mounted in the line.

Once the desired pressure was obtained, the valve between the gas supply tank and the surge tank was closed. The volume of the surge tank was large enough so that gas flow through the section would not decrease the line pressure. Should a tube failure occur, only the surge tank volume would be introduced into the detection system.

## 3. Flow Detection System

The flow rates through the section were measured with a Veeco GA-4 residual gas analyzer (R.G.A.). The R.G.A. was mounted on a stainless steel tank connected directly to a turbomolecular pump. The vacuum system also pumped on the space between the specimen and the alumina protection tube. Gas permeating through the section into the protection tube is drawn into the tank where it is monitored by the R.G.A. The analyzer output is displayed as a trace on a 3-decade linear recorder.

Standardization of the analyzer was accomplished by introduction of helium or argon sources of known leak rate into the system. Sensitivity was calculated in terms of atoms per second per division. Accuracy of the standard leaks was supposedly within  $\pm 10\%$  of the rate quoted by the suppliers.



### C. Test Procedure

#### 1. General Procedure.

All specimens were heated to the maximum test temperature under vacuum and held for at least 12 hours to outgas the system. Runs were begun at the highest temperature with subsequent reduction in temperature for each new data point.

Gas pressures were increased in successive runs on each tube.

All helium runs were made first, followed by the argon tests.

#### 2. Helium Procedure.

Runs using helium pressures of 380, 760, and 1010 mm Hg were made. Tests were made over temperature ranges of 1300-800°C and 1525-850°C for the 94 and 99.5% Al<sub>2</sub>O<sub>3</sub> specimens, respectively.

Elapsed time between introduction of the gas into the system and measurement of the helium peak height (mass to charge ratio = 4) and background to either side of the helium peak was equal to, or longer than, the length of time for flow through the section to come to a constant value. This required 12 to 24 hours, depending on the temperature, and the composition of the tube.

After helium peak height and background readings were taken, the valve from the analyzer tank to the sample chamber was closed. The standard leak was then admitted to the tank and a sensitivity calibration was made. The standard leak was kept at one temperature during all calibrations since the leak rate varies with temperature.

After standardization, the valve to the sample was reopened and the temperature was lowered. When enough time had elapsed for the flow rate to become constant once again (6.5-8 hrs.), new readings and calibrations

were made.

After readings were completed at the lowest temperature, the test pressure was increased. The temperature was once again raised to the maximum and the entire procedure of constant flow rate, reading, and calibration was repeated.

The output of the R.G.A. was recorded in either of two ways. In the first, the R.G.A. was set on the helium peak maximum. Checks were made to make sure the maximum peak height was being recorded. Drift in background on both sides of the helium peak was also checked and recorded. Both checks were made just prior to the final measurement.

Secondly, the output could be displayed as a continuous series of peaks. By impressing a ramp function voltage onto the ion analyzer section of the R.G.A. it was possible to slowly sweep back and forth over the gas peak. Thus, a series of peak height and background points was obtained, from which the appropriate data could be taken.

## 2. Argon Procedure.

The 99.5%  $\text{Al}_2\text{O}_3$  specimen was tested at argon pressures of 510 mm Hg, 760 mm Hg, and 1010 mm Hg at temperatures of  $1475^\circ\text{C}$  and  $1254^\circ\text{C}$ ; the 94%  $\text{Al}_2\text{O}_3$  tube at 760 mm Hg at  $1283^\circ\text{C}$ .

There were large changes in testing procedure for the argon runs due to the argon content in the air. With helium, the peak height at mass to charge ratio ( $m/e$ ) = 4 would reduce to the overall background rate if no helium was permeating through the sample and the valve to the standard leak was closed. With argon, however, there was a definite background peak at  $m/e = 40$  (the argon peak) from the specimen chamber and the analyzer tank. This peak apparently was due to the argon

content in air at the pressures obtained by the vacuum system, and to outgasing of the analyzer tank. Slight air leakage did occur through the rubber "O"-rings sealing the specimen in the envelope tube. The background peak at  $m/e = 40$  changed slightly with time and varied with the temperature of the specimen.

Once argon was admitted to the inside of the specimen, one could not be sure whether the peak height at  $m/e = 40$  measured was argon background or argon background plus some flow rate through the tube. Thus only one background measurement could be made--just prior to the introduction of the argon into the specimen.

The 99.5%  $Al_2O_3$  specimen was heated in vacuum for 60 hrs. at  $1472^\circ C$  to reduce the helium content in the section and measure the variation of the background peak (specimen tube + analyzer tank) at  $m/e = 40$ . An argon pressure of 510 mm Hg was admitted. The peak was monitored for 46 hrs. At that time final peak height readings of the tube + tank, leak + tank, and tank alone were taken. The argon pressure was raised to 760 mm Hg. After 26 hrs., another set of readings was taken. This was repeated once again for 1010 mm Hg of argon.

The specimen was then put under vacuum at  $1475^\circ C$  for 60 hrs. The temperature was lowered to  $1253^\circ C$  where once again the tube + tank background variation at  $m/e = 40$  was monitored for 40 hours. Argon pressures of 510, 760, and 1010 mm Hg were again successively introduced and the same three peak heights measured, each time after 24 hrs. at temperature.

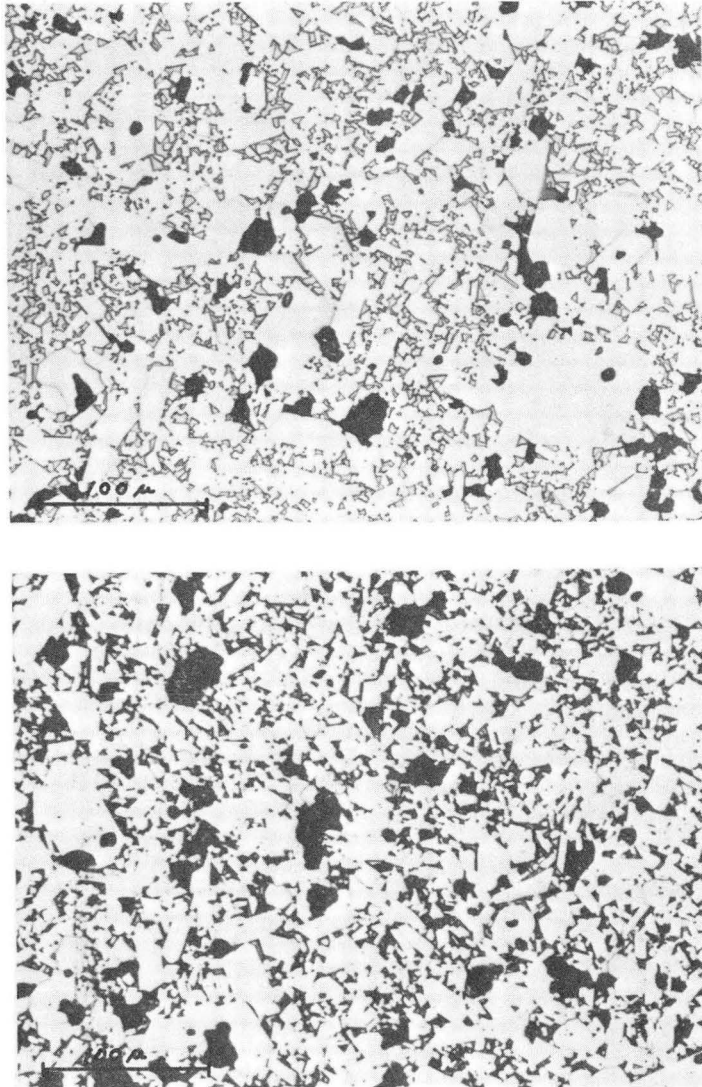
The 94%  $Al_2O_3$  specimen was tested in the same way except only one temperature ( $1277^\circ C$ ) and one pressure (760 mm Hg) was used.

D. Microscopic Examinations

Polished sections were made of the as-received materials but no attempt was made at a detailed microstructure study. Sections were cut from the materials with a diamond saw and mounted in clear casting resin. The surface was recut with the saw after mounting. The sections were ground on a 50 micron bonded diamond lap. Polishing was done by 30 micron diamond paste followed with a water slurry of Linde A alumina. Etching was done in hot (190-210°C) orthophosphoric acid for 2-6 minutes. A gold film was vapor deposited on the polished surfaces to eliminate internal reflections.

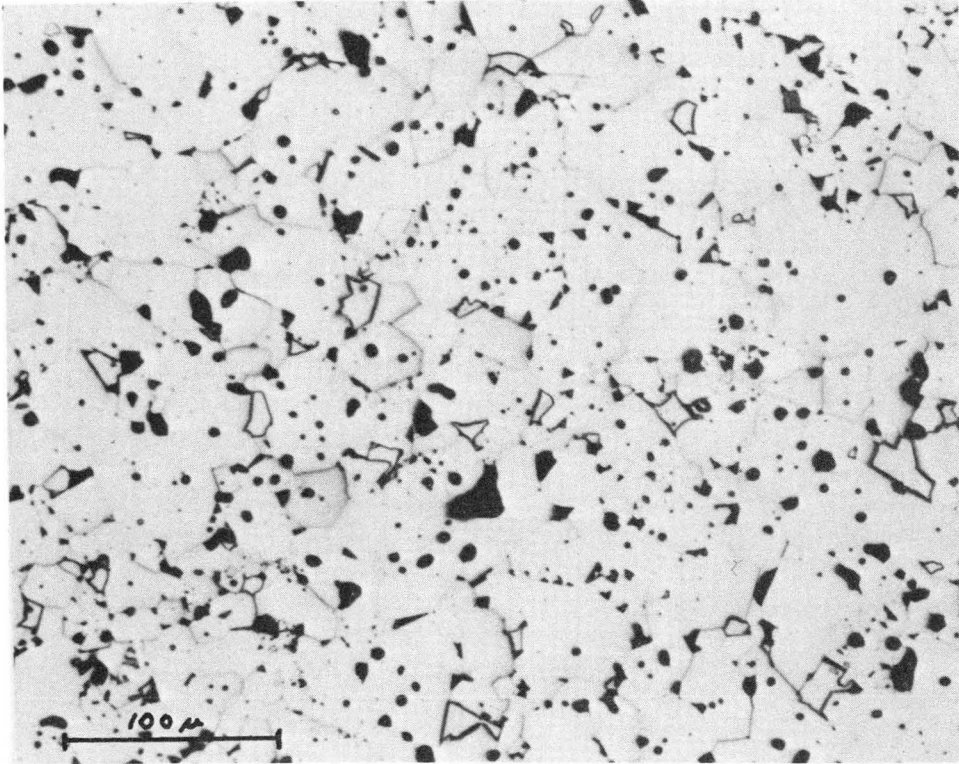
Particle size ranges of 3-110, and 15-80 microns were found in the 94 and 99.5% Al<sub>2</sub>O<sub>3</sub> as-received materials; respectively (Figs. 6 and 7). The glassy phase was clearly visible in the 94% Al<sub>2</sub>O<sub>3</sub> material. It could not be determined microscopically whether the glass was a complete matrix material for the alumina particles, or whether it occurred as discrete pockets of glass. In the 99.5% Al<sub>2</sub>O<sub>3</sub> material, discrete impurity-phase areas could be seen.

Polished sections of the materials after testing were not available for study.



ZN-5897

Fig. 6. Photomicrographs of as-received 94% Al<sub>2</sub>O<sub>3</sub> material (a) before etching and (b) after etching.



ZN-5898

Fig. 7. Photomicrograph of as-received 99.5% Al<sub>2</sub>O<sub>3</sub> material after etching.

#### IV. EXPERIMENTAL RESULTS

##### A. Helium Permeation Constants

The permeation constant,  $K$ , in units of atoms/sec cm atm, was calculated using the method outlined in Appendix I. The flow rate data and the calculated permeation constants for each specimen are tabulated in Tables V and VI, Appendix II. Semilog plots of the permeation constant versus  $1/T(^{\circ}K^{-1})$  are presented in Figs. 8 and 9. A comparison of the permeation constants at 760 mm Hg helium pressure for the two materials is shown in Fig. 10.

The  $K$  values for specimen #1 are at least 15 times higher than for the higher alumina content material. The decrease of  $K$  with temperature appears approximately the same for both tubes.

##### B. Helium Activation Energies

Activation energies for the permeation of helium through alumina were calculated by a linear regression of  $\ln K$  on  $1/T(^{\circ}K^{-1})$ . A confidence limit of 95% was used. The resulting activation energies are listed in Table IV. The average activation energies are  $13.6 \pm 2.3$ , and  $13 \pm 1.7$  Kcal/mole for the 94 and 99.5%  $Al_2O_3$  specimens, respectively. Within the confidence limits listed, there is no difference in the activation energies calculated for the 94 and 99.5%  $Al_2O_3$  specimens.

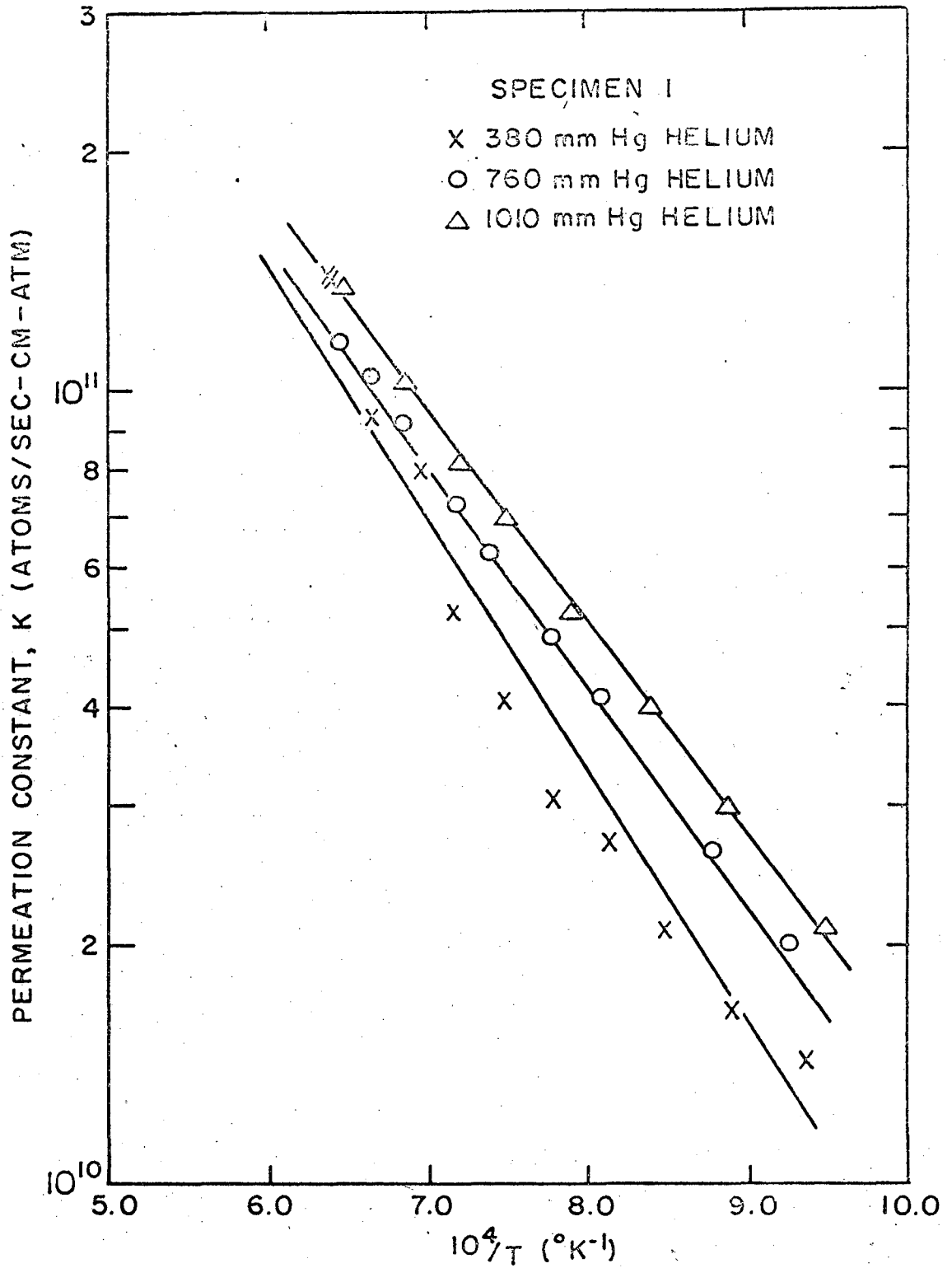


Fig. 8. Temperature dependence of the permeation constant for Specimen 1, 94%  $Al_2O_3$ .



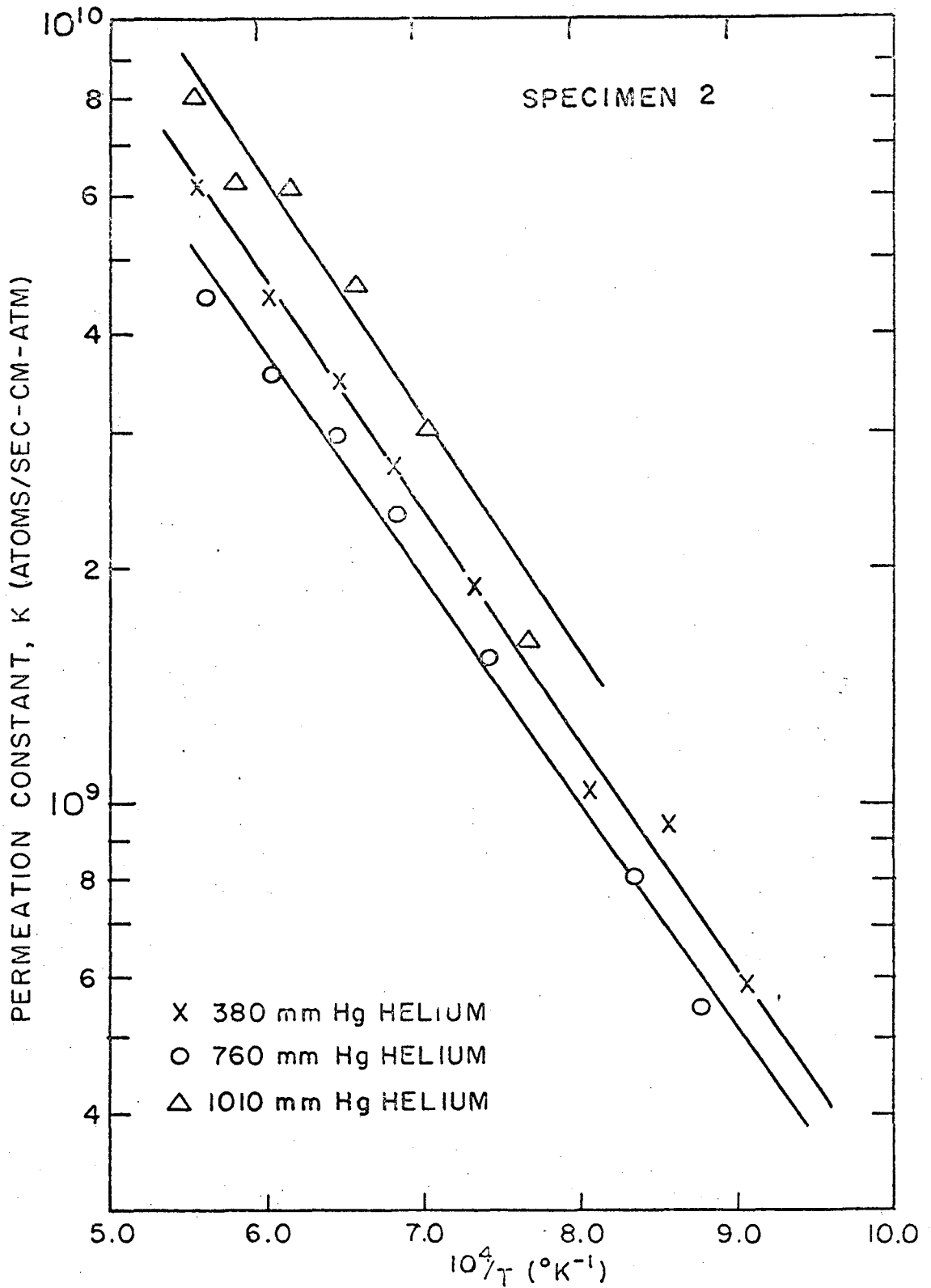


Fig. 9. Temperature dependence of the permeation constant for specimen 2, 99.5%  $\text{Al}_2\text{O}_3$ .

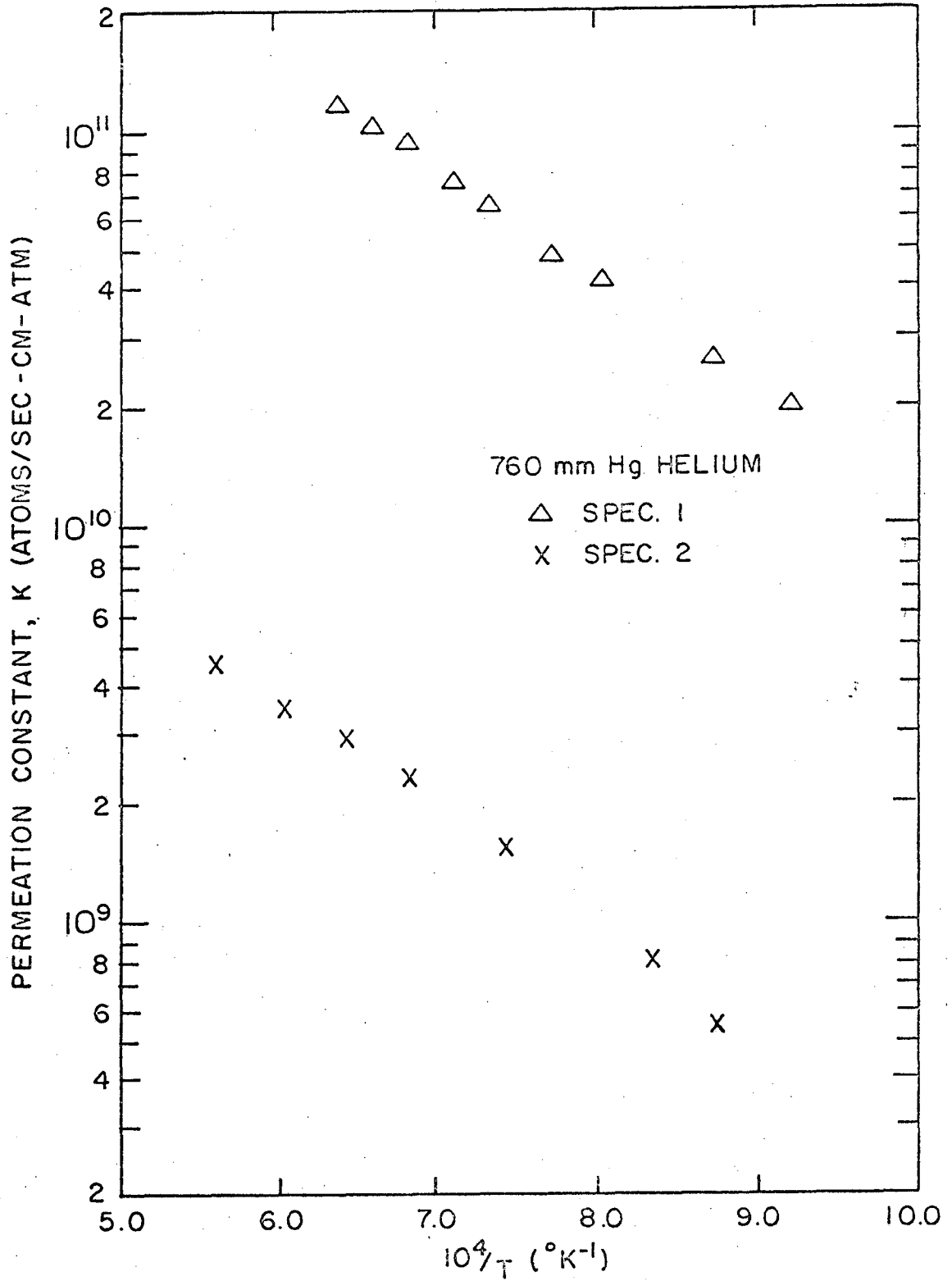


Fig. 10. Comparison of the permeation constants for Specimens 1 and 2 at 760 mm Hg helium pressure.

Table IV. Activation energies for helium permeation

Spec. #	Composition (% Al <sub>2</sub> O <sub>3</sub> )	Pressure (mm Hg)	Activation Energy (Kcal)
1	94	380	13 ± 1.8
		760	13 ± 1.5
		1010	15 ± 3.5
2	99.5	380	15 ± 2.0
		760	12 ± 1.5
		1010	12 ± 1.5

C. Argon Permeation Runs

To be significant, it was judged that a peak height reading must be at least twice as large as the argon background variation with time of the tank plus specimen tube chamber. In no case during the argon runs with either specimen were any significant data points found. The data recorded for the experiments are tabulated in Table VII, Appendix II.

A lower limit of K detectability was calculated from the requirements for a significant reading and the R.G.A. argon sensitivity. The minimum K which could be measured in these experiments was found to be  $\approx 2 \times 10^9$  atoms/sec cm atm. Thus, the permeation constant for argon in the 94 and 99.5% Al<sub>2</sub>O<sub>3</sub> specimens must be less than  $2 \times 10^9$  atoms/sec cm atm in the temperature range used.

## V. DISCUSSION

The permeation constants,  $K$ , for the 99.5%  $\text{Al}_2\text{O}_3$  material agree to within a factor of 3 with the results of Rose<sup>10</sup> who used similar material but a different gas analyzing system. The calculated activation energies are also in agreement. The 99.5%  $\text{Al}_2\text{O}_3$  tubes used in this study and those used by Rose are from the same manufacturer but from different lots ordered 2 years apart. Frequently different ceramic tubes of the same composition exhibit non-reproducible permeation behavior.<sup>7</sup> The fact that these results agree indicates that the manufacturer is maintaining close control of the processing of this body, which all producers of ceramics must do if reliable, reproducible products are to be obtained.

Helium is known to permeate through glasses at high rates in comparison with inorganic crystalline material.<sup>16</sup> It would be expected from consideration of glass content alone that specimen 1 would show the highest permeation rate at a given temperature if glassy phase paths exist through the body. Permeation rates 15 times that of the other body were observed.

If diffusion through a glassy phase is rate controlling, then the activation energy for the permeation process should correspond with the permeation activation energies reported for helium through glass. An average activation energy of  $13.6 \pm 2.3$  was found for the 94% alumina specimen in this study. Norton<sup>17</sup> and Altemose<sup>18</sup> have studied permeation of helium through commercial glass compositions. Each has found activation energies for helium permeation up to 12.4 Kcal/mole, which are in reasonable agreement with the values obtained in this experiment.

Besides helium diffusion through glassy paths, another diffusion mechanism is possible. This is diffusion along true alumina-alumina grain boundaries. No reliable activation energy data for either diffusion or permeation of helium along alumina grain boundaries is available. Helium diffusion through polycrystalline metals, however, has been studied. Diffusion activation energies of 39 and 36.5 Kcal/mole have been found for magnesium<sup>19</sup> and aluminum,<sup>20</sup> respectively. The activation energy for permeation is the sum of the activation energies for diffusion and solution. Therefore, the activation energy for permeation through the metals would be higher than those given for diffusion. Since these permeation activation energies would surely be greater than 40 Kcal/mole, it seems unlikely that permeation through Al<sub>2</sub>O<sub>3</sub> along true alumina-alumina grain boundaries would have as low an activation energy as 13 Kcal/mole. It would appear then that the most probable mechanism for helium permeation is diffusion through a continuous glassy phase.

An average activation energy of  $13 \pm 1.7$  Kcal/mole was found for the specimen 2, 99.5% Al<sub>2</sub>O<sub>3</sub>. Here again, diffusion through some glassy path must be considered the most probable permeation mechanism, as the activation energies are in agreement with such a prediction. One cannot say such a glassy layer exists on the basis of photomicrographs of these samples; however, it is possible that a continuous glassy or amorphous layer is still present in the body. Kingery<sup>21</sup> has speculated that such a thin glassy layer exists in ceramic compositions of the purity used in this experiment (>99%). This microstructural distribution of phases cannot be detected by current microstructural analysis techniques.

The approximate amount and composition of the glassy phase which exists in the fired body can be determined. If one assumes equilibrium is attained at the firing temperature and the liquid phase present forms a glass on cooling with some exsolution of the primary phase, the necessary information can be obtained from the appropriate phase diagram. Using composition data from the spectrographic analysis, the glass composition of the 99.5%  $\text{Al}_2\text{O}_3$  specimen was calculated to be 26, 14 and 60 weight percent  $\text{SiO}_2$ ,  $\text{MgO}$ , and  $\text{Al}_2\text{O}_3$ , respectively. The liquid portion was 1.15 weight percent of the body. Assuming the liquid on cooling to a glass would be 85% of the theoretical crystalline density, the glass content would be 1.6% by volume. This amount of glass should be enough to form continuous glassy paths through the body.

The 94%  $\text{Al}_2\text{O}_3$  body contains 3 major impurities-- $\text{SiO}_2$ ,  $\text{MgO}$ , and  $\text{CaO}$ . No quaternary phase diagrams in the area of interest are available, but the ternary diagrams for  $\text{Al}_2\text{O}_3$  and  $\text{SiO}_2$  with the two RO compounds are very similar. Reasonable information can be obtained by consulting both diagrams, first considering the RO impurity to be all  $\text{CaO}$ , and then all  $\text{MgO}$ . The range of composition found was 40-44%  $\text{SiO}_2$ , 44-49%  $\text{Al}_2\text{O}_3$ , and 11-12%  $(\text{CaMg})\text{O}$ . The glass content on cooling was calculated to be 12-13 volume percent of the body.

The apparent glass compositions of both bodies contain very low amounts of silica, the glass-forming oxide present. Altemose<sup>18</sup> and Norton<sup>17</sup> found a relationship between the amount of glass-former and the activation energy for helium permeation. The lower the amount of glass-former present, the higher the activation energy. From Norton's results, using glasses containing as little as 22 weight percent glass-

formers, one would expect an activation energy of approximately 13 Kcal/mole for both compositions used in this study. An extrapolation of Altemose's data predicts higher activation energies, 17 and 22 Kcal/mole for the 94 and 99.5%  $\text{Al}_2\text{O}_3$  bodies, respectively. However, his data only extends to compositions containing greater than 55 weight percent glass-former. The maximum activation energy he reported was 12.4 Kcal/mole.

Although the activation energies for helium permeation through specimens 1 and 2 are similar, the apparent diffusion coefficient at a given temperature through the 99.5 specimen is considerably smaller than that for the 94%  $\text{Al}_2\text{O}_3$  sample.

The apparent diffusion coefficient is inversely proportional to the lag time.<sup>22</sup> After introduction of the gas into the specimen tube, some time elapses before gas flow is detected. The flow rate increases slowly at first and then reaches a constant rate of increase. Finally the rate of increase falls and a constant flow rate is reached. The lag time is defined as the time where the extrapolation of the constant rate of increase portion of the curve of flow rate vs. time intersects the time axis. The lag time for the 94%  $\text{Al}_2\text{O}_3$  specimen was 42 minutes at 1300°C, while for the 99.5%  $\text{Al}_2\text{O}_3$  tube it was nearly 5 hours at 1500°C. Thus, with new tubes of a given thickness at a given temperature, the 99.5%  $\text{Al}_2\text{O}_3$  material would appear impermeable to helium for a much greater length of time than the 94% material.

The argon permeation experiments demonstrate the extreme dependence of the size of the permeating specie on permeation through alumina ceramics. The minimum detectability of the residual gas analyzer

differed by approximately one order of magnitude for helium and argon. The minimum helium detectability was approximately  $4 \times 10^{10}$  atoms per sec. flowing through the system; for argon this value was  $3.5 \times 10^{11}$  atoms per sec. Helium was observed to flow through the 94% alumina ceramic at a maximum rate of  $3 \times 10^{13}$  atoms per sec. at  $1275^{\circ}\text{C}$  under a pressure difference of 1010 mm of Hg. At approximately the same temperature and a pressure of 760 mm Hg of argon, no detectable flow was observed. Therefore, the argon permeation rate is at least 100 times less than the rate for helium. The radius of the helium and argon atoms are given as  $0.93\text{\AA}$  and  $1.54\text{\AA}$  respectively. Similar helium-argon size effects have been found in permeation through glasses. Norton<sup>16</sup> reported changes between helium and argon permeation constants by a factor of greater than  $2 \times 10^7$  atoms/sec cm atm in silica glass. Similar changes in the permeation rates through the alumina materials would have resulted in values of K in the  $10^4$  atoms/sec cm atm range, or roughly a factor of  $10^5$  lower than the limit of detectability in this system.



## VI. SUMMARY AND CONCLUSIONS

Permeation studies of helium and argon through commercial polycrystalline alumina bodies were made. Permeation occurred through thin diamond ground cylindrical sections approximately 0.035 inches thick and 0.375 inches in diameter. Flow rates were measured by a residual gas analyzer. The analyzer was standardized by introducing a calibrated leak into the system.

Helium pressures of 380 to 1010 mm Hg over temperatures from 783 to 1539°C were used for specimens containing 94 and 99.5 weight percent  $\text{Al}_2\text{O}_3$ . Calculated helium permeation constants up to  $1.4 \times 10^{11}$  and  $8.1 \times 10^9$  atoms/sec cm atm and average activation energies for helium permeation of  $13.6 \pm 2.3$  and  $13 \pm 1.7$  Kcal/mole were found for the 94 and 99.5%  $\text{Al}_2\text{O}_3$  specimens, respectively.

The most probable flow mechanism for helium permeation through the 94 and 99.5%  $\text{Al}_2\text{O}_3$  materials used in this study is diffusion through continuous glassy phase paths in the body. This is based on activation energy comparisons for helium permeation through glasses.

Permeation was found to be dependent on the size of the permeating gas specie. No argon flow through either alumina composition was detected at argon pressures to 1010 mm Hg and temperatures to 1475°C. The limit of detectability of the apparatus fixes K values for argon permeation at less than  $2 \times 10^9$  atoms/sec cm atm in the temperature range studied.

ACKNOWLEDGMENTS

The author wishes to gratefully acknowledge the valuable guidance and aid of Professor R. M. Fulrath during the course of this investigation.

He is grateful to his fellow graduate students for their suggestions and encouragement, and to Dr. J. P. Roberts for helpful discussions.

In addition, he is indebted to Mr. George Dahl for preparation of the photomicrographs.

This work was done under the auspices of the Atomic Energy Commission.

Appendix I. Method of Determination  
of Permeation Constant, K.

The permeation constant, K (atoms/sec cm atm), relates the steady state gas flow rate, q (atoms/sec), thickness, t(cm), and area, A(cm<sup>2</sup>) of the sample, and pressure differential, ΔP (atm) across the specimen as given in the equation

$$q = K \frac{A}{t} (\Delta P)$$

With cylindrical specimens, the most realistic area to use in calculations is the effective area,  $A \left[ \frac{k-1}{\ln k} \right]$ , as used by Rose<sup>10</sup> and Stansfield,<sup>9</sup> where

A = Inside area of permeation section, cm<sup>2</sup>

k = Inside radius/outside radius of section

The steady state flow rate through the membrane is measured by the residual gas analyzer. The relationship between the flow rate, q, and the R.G.A. output is given by

$$q = hs'$$

where h = residual gas analyzer output (div.)

s' = sensitivity of residual gas analyzer (atoms/sec. div.)

The permeation coefficient, K, is thus obtained from the R.G.A. output by using the equation

$$K = \frac{hs't}{\left[ A \left( \frac{k-1}{\ln k} \right) \right] \Delta P}$$

where all symbols have their previous meaning.

Appendix II. Experimental Data and Calculated Permeation Constants.

Table V. Helium permeation data and permeation constants for specimen 1, 94% Al<sub>2</sub>O<sub>3</sub>.

Pressure (mm Hg)	Temp. (°C)	R.G.A. peak height, h (div.)	R.G.A. sensitivity, s' (atoms/sec.div.) x10 <sup>-12</sup>	Flow rate, q (atoms/ sec.) x10 <sup>-12</sup>	Permeation constant, K (atoms/ sec.cm atm) x10 <sup>-10</sup>
380	1301	9.2	1.250	11.5	14
	1238	6.5	1.178	7.66	9.2
	1170	5.6	1.169	6.55	7.9
	1131	3.5	1.243	4.35	5.2
	1065	2.7	1.233	3.33	4.0
	1016	2.2	1.149	2.53	3.0
	962	1.8	1.243	2.24	2.7
	918	1.4	1.253	1.75	2.1
	853	1.1	1.253	1.38	1.7
	797	0.96	1.264	1.21	1.5
	1302	8.8	1.289	11.3	14
	760	1286	15.26	1.247	19.0
1237		13.54	1.260	17.1	10.3
1191		11.70	1.292	15.1	9.13
1129		9.51	1.253	11.9	7.20
1082		8.12	1.267	10.3	6.21
1019		6.45	1.243	8.02	4.84
964		5.29	1.274	6.74	4.07
867		3.50	1.240	4.34	2.62
809		2.63	1.253	3.29	1.99
1010		1275	25.25	1.167	29.5
	1190	18.89	1.297	22.5	10.2
	1119	14.77	1.200	17.7	8.05
	1064	12.80	1.185	15.2	6.89
	996	9.88	1.176	11.6	5.28
	923	7.42	1.185	8.79	3.99
	856	5.65	1.164	6.58	2.99
	783	4.01	1.152	4.62	2.10

Table VI. Helium permeation data and permeation constants for specimen 2, 99.5% Al<sub>2</sub>O<sub>3</sub>

Pressure (mm Hg)	Temp. (°C)	R.G.A. peak height (div.)	R.G.A. sensitivity atoms/sec.div. x10 <sup>-12</sup>	Flow rate, q (atoms/ sec.) x10 <sup>-12</sup>	Permeation constant, K (atoms/ sec. cm atm.) x10 <sup>-9</sup>
380	1524	0.51	1.089	5.55	6.2
	1394	0.37	1.087	4.02	4.5
	1274	0.29	1.084	3.14	3.5
	1195	0.23	1.066	2.45	2.7
	1095	0.16	1.061	1.70	1.9
	968	0.09	1.037	0.933	1.0
	895	0.08	1.066	0.853	0.95
	834	0.05	1.057	0.528	0.59
760	1508	0.77	1.049	8.08	4.5
	1382	0.62	1.023	6.35	3.5
	1276	0.50	1.064	5.32	2.9
	1191	0.38	1.069	4.18	2.3
	1071	0.26	1.098	2.78	1.5
	926	0.14	1.031	1.44	0.80
	867	0.09	1.089	0.980	0.54
	1010	1539	1.33	1.461	19.4
1451		1.03	1.457	15.0	6.2
1361		0.91	1.633	14.9	6.1
1256		0.67	1.652	11.1	4.6
1149		0.42	1.714	7.20	3.0
1031		0.22	1.753	3.86	1.6

Table VII. Peak height data for argon permeation runs

Spec #	Temp. °C	Pressure (mm Hg)	Time at temp. (hrs)	R.G.A. peak height (div.)	
				Background variation tank & tube	Tank & tube after permeation run
2	1472	-	40	21.6-22.6	-
	1473	510	46		21.7
	1473	760	26		22.7
	1475	1010	24		22.6
2	1253	-	40	21.9-22.7	-
	1253	510	44		22.6
	1254	760	24		21.9
	1254	1010	24		22.1
1	1283	-	40	32.5-33.6	-
	1277	760	24		32.5

REFERENCES

1. D. Hayes, D. W. Budworth, and J. P. Roberts, "Selective Permeation of Gases through Dense Sintered Alumina," *Trans. Brit. Ceram. Soc.*, 60, (7), 494-504 (1961).
2. D. Hayes, D. W. Budworth, and J. P. Roberts, "Permeability of Sintered Alumina Materials to Gases at High Temperatures," *Trans. Brit. Ceram. Soc.*, 62, [6], 507-523 (1963).
3. G. M. Fryer, D. W. Budworth, and J. P. Roberts, "The Influence of Microstructure on the Permeability of Sintered Alumina Materials to Gases at High Temperatures," *Trans. Brit. Ceram. Soc.*, 62, (6), 525-536 (1963).
4. J. P. Roberts, "Microstructural Considerations in Gas Permeation," Ceramic Microstructures, Chapter 25, J. Wiley and Sons (in press).
5. E. W. Roberts and J. P. Roberts, "The Mechanism of Permeability of Ceramics to Gases," U.K.A.E.A. Agreement No. 13/5/165/1394. Progress Report No. 7 (1 July-31 December 1964).
6. A. K. Dhavale and J. P. Roberts, "Formation of Connected Porosity in Dense Oxide Ceramics after Prolonged Heating at High Temperature," Ceramics Division, Houldsworth School of Applied Science, University of Leeds, Progress Report No. 5 (1 January 1965-30 June 1965).
7. H. F. Volk and F. W. Meszanos, "Oxygen Permeation through Alumina; Influence of Microstructure and Purity," Ceramic Microstructures, Chapter 33, J. Wiley and Sons (in press).
8. W. B. Campbell, "Diffusion Rate and Activation Energy of Helium through Single Crystal and Polycrystalline Alumina," (M.S. Thesis), Georgia Institute of Technology, 1960.

9. O. M. Stansfield, "The Influence of Tensile Stress on Gaseous Permeation in Glassy-State and Complex Ceramics," (M.S. Thesis), UCRL-10755, April 1963.
10. R. E. Rose, "Permeation of Gases through Alumina," (M.S. Thesis), UCRL-16017, April 1965.
11. P. L. Studt, "Mechanism of Gaseous Permeation through Glass, Single-Crystal Silicon, Germanium; and Stress-Enhanced Gaseous Permeation through Alumina Bodies," (Ph.D. Thesis), UCRL-10466, September 1962.
12. A. E. Atallah, "Effect of Stress on Permeation through Alumina Membranes," (M.S. Thesis), UCRL-11355, April 1964.
13. G. M. Fryer and J. P. Roberts, "Development of Gas-Permeability in Sintered Alumina during Tensile Creep," Science of Ceramics, (Academic Press for the British and Netherlands Ceramic Societies), Vol. 3 (in press).
14. D. W. Budworth, E. W. Roberts, and W. D. Scott, "Joining of Alumina Components by Hot-Pressing," Trans. Brit. Ceram. Soc., 62 [10], 949-954 (1963).
15. R. C. Rossi, "The Kinetics and Mechanism of Final Stage Densification in the Vacuum Hot-Pressing of Fine-Grained Aluminum Oxide," (Ph.D. Thesis), UCRL-11564, July 1964.
16. F. J. Norton, "Permeation of Gases through Solids," J. App. Phys., 28, (1) 34-39 (1957).
17. F. J. Norton, "Helium Diffusion Through Glass," J. Am. Ceram. Soc., 36 90-96 (1953).
18. V. O. Altemose, "Helium Diffusion through Glass," J. App. Phys., 32 (7), 1309-1316 (1961).



19. H. R. Glyde and K. I. Mayne, "Helium and Argon Diffusion in Magnesium," *Phil. Mag.*, 12 (119) 919-938 (1965).
20. H. R. Glyde and K. I. Mayne, "Helium Diffusion in Aluminum," *Phil. Mag.*, 12 (119) 997-1004 (1965).
21. W. D. Kingery, Introduction to Ceramics, J. Wiley & Sons, New York (1960), p. 243.
22. R. M. Barrer, Diffusion in and through Solids, Cambridge Univ. Press, London (1941), p. 418.

This report was prepared as an account of Government sponsored work. Neither the United States, nor the Commission, nor any person acting on behalf of the Commission:

- A. Makes any warranty or representation, expressed or implied, with respect to the accuracy, completeness, or usefulness of the information contained in this report, or that the use of any information, apparatus, method, or process disclosed in this report may not infringe privately owned rights; or
- B. Assumes any liabilities with respect to the use of, or for damages resulting from the use of any information, apparatus, method, or process disclosed in this report.

As used in the above, "person acting on behalf of the Commission" includes any employee or contractor of the Commission, or employee of such contractor, to the extent that such employee or contractor of the Commission, or employee of such contractor prepares, disseminates, or provides access to, any information pursuant to his employment or contract with the Commission, or his employment with such contractor.